

GMM-Based Generative Adversarial Encoder Learning

Yuri Feigin, Hedva Spitzer and Raja Giryes
 School of Electrical Engineering
 Tel Aviv University
 Israel, 69978

{yurifeigin@mail, hedva@tauex, raja@tauex}.tau.ac.il

Abstract

While GAN is a powerful model for generating images, its inability to infer a latent space directly limits its use in applications requiring an encoder. Our paper presents a simple architectural setup that combines the generative capabilities of GAN with an encoder. We accomplish this by combining the encoder with the discriminator using shared weights, then training them simultaneously using a new loss term. We model the output of the encoder latent space via a GMM, which leads to both good clustering using this latent space and improved image generation by the GAN. Our framework is generic and can be easily plugged into any GAN strategy. In particular, we demonstrate it both with Vanilla GAN and Wasserstein GAN, where in both it leads to an improvement in the generated images in terms of both the IS and FID scores. Moreover, we show that our encoder learns a meaningful representation as its clustering results are competitive with the current GAN-based state-of-the-art in clustering.¹

1. Introduction

Generative adversarial networks (GAN) are a powerful tool that allows learning data distributions and is widely used in many fields [16, 32, 27, 37, 41, 28, 56, 7, 24, 18, 29, 22, 6]. Despite their great success, GANs still suffer a few notable limitations.

First, the distribution of the generated data still does not match the distribution of the real one. In almost every application, GANs will generate at least some outputs that appear obviously synthetic. Many GAN training techniques are unstable, as they lack a mechanism that can autonomously stop the training upon a point of convergence, rather than upon some point decided by human intervention. The problem

of mode collapse, or partial mode collapse, also still remains unsolved: while GAN successfully generates some parts of the data distribution, there are other parts that it does not generate. Furthermore, although the GAN generator can create high quality outputs, most GANs do not supply a mechanism that can take the output and infer its latent representation, which could be very helpful for unsupervised learning. This last point constitutes a particularly acute limitation. If the network cannot infer a latent space, then it is excluded from a number of applications involving an encoder.

This paper explores whether it is possible to successfully incorporate an encoder with GAN. To do so, we present GMM-based generative adversarial encoder learning (GAEL), a hybrid GAN-Encoder network. While GAEL demonstrates improved performance on different GANs, its method is fairly simple. It consists of adding to the GAN an encoder, which shares most of its weights with the discriminator (or critic in WGAN). Then we train the encoder using a simple loss that is added to the regular GAN loss. The shared weights and simple loss mean that the network's innovations come with very little computational overhead or additional training time. After training finishes, we fit the outputted latent space of the real images to a Gaussian Mixture Model (GMM). Then we sample latent vectors from the GMM and use them as the generator input for generating synthetic images.

We evaluate GAEL on three important applications related to GANs: image reconstruction, image generation, and clustering. To examine how well our encoder learns meaningful representation, we decode the latent space images and compare the reconstructions to the originals (there is no use of GMM at this stage). Then, we use our encoder to learn a new distribution (GMM) to replace the original one used for the generator input during training. We then test how well the network generates images from the new latent distribution. Fi-

¹Source code will be released upon publication.

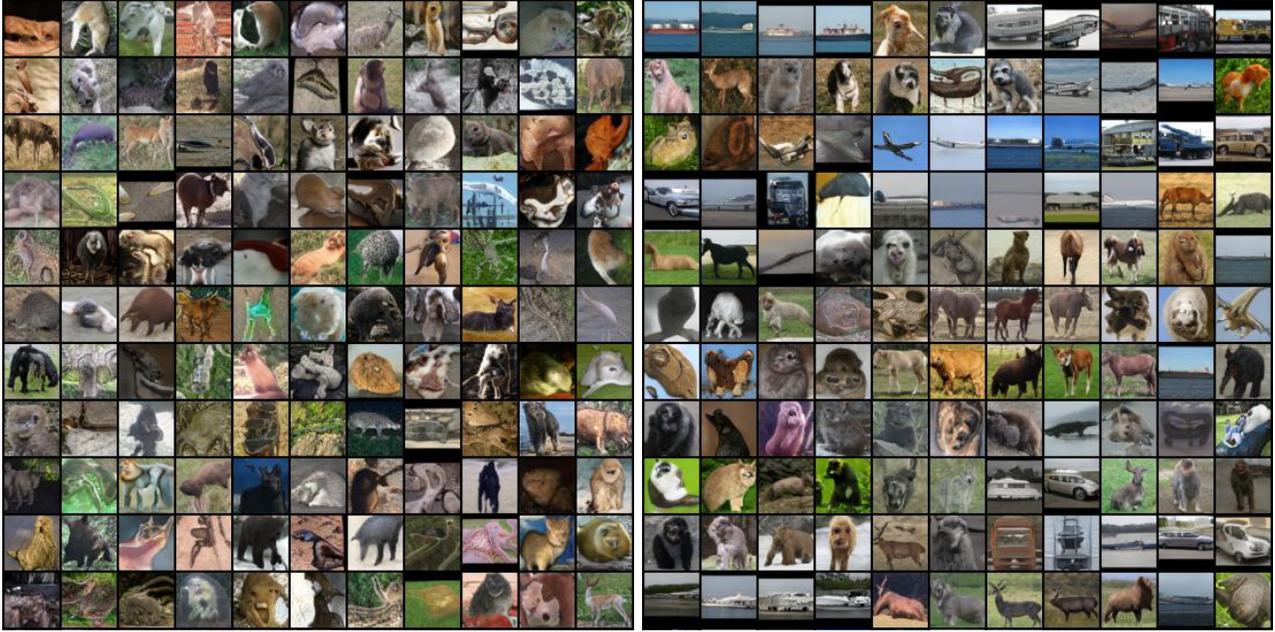


Figure 1: Unsupervised image generation (without labels) on STL-10: (left) baseline WGAN; (right) GAEL. GAEL, which shares the same generator and discriminator like the baseline exhibits much more realistic images with meaningful semantic information. Images chosen randomly.

nally, we test how well our network clusters. We do this by fitting the GMM to the latent space, using GMM modes as proxies for dataset labels, i.e., each Gaussian in the GMM is assumed to represent a class in the data.

In our experiments, we use a variety of datasets including MNIST, CIFAR-10, CIFAR-100, CelebA, STL-10, and Imagenet. We use both quantitative and qualitative methods to evaluate the results. For metric assessment, we evaluate our image generation results with inception(IS) [52] and Frechet Inception Distance (FID) [25] scores, and our clustering results with the Adjusted Rand Index (ARI), Normalized Mutual Information (NMI), and clustering Accuracy (ACC) [61].

On all datasets and evaluation metrics, our strategy performs very well. Our GMM-based GAN generates better images than those generated using its baselines and many other unsupervised image generation techniques. The network’s clustering performance is competitive with the results of the CNN-based clustering and, as far as we know, better than current GAN-based techniques.

In summary, this paper introduces GAEL, a hybrid GAN-Encoder framework. The GAN and the Encoder train simultaneously, and the encoder and discriminator share weights throughout nearly the entire training. The method performs robustly on multiple datasets. We summarize GAEL’s contributions as follows: (i) It improves how GAN performs at image reconstruc-

tion, clustering and image generation; (ii) the method is generic, and can be ported to other architectures; (iii) the encoder could likely help improve future GAN implementations; and (iv) it stabilizes training.

2. Related Work

The research that has been performed on GANs is vast. Since the seminal work by Goodfellow et al [20], there have been significant attempts to improve the performance of GANs. The improvements have been developed through a variety of means, including through improved architectural structure [4, 12, 11, 31, 49, 64, 34], the introduction of labelled data to improve performance [43, 30, 57, 45, 9], and on to different loss functions [2, 21, 46, 59, 44, 47]. For example, some works add a maximum-mean-discrepancy loss to improve GAN training [39, 58]. Other approaches use reconstruction loss to optimize the generator without a discriminator [5, 26]. Other approaches used architecture search to find the generator architecture [19, 14, 54, 55].

In general, GANs generate images from a given latent distribution. Yet, the other direction is usually not present, i.e., getting representation that leads to the generation of a given image as provided in auto-encoders [36, 13]. Calculating such a representation is useful for unsupervised learning, e.g., using the latent

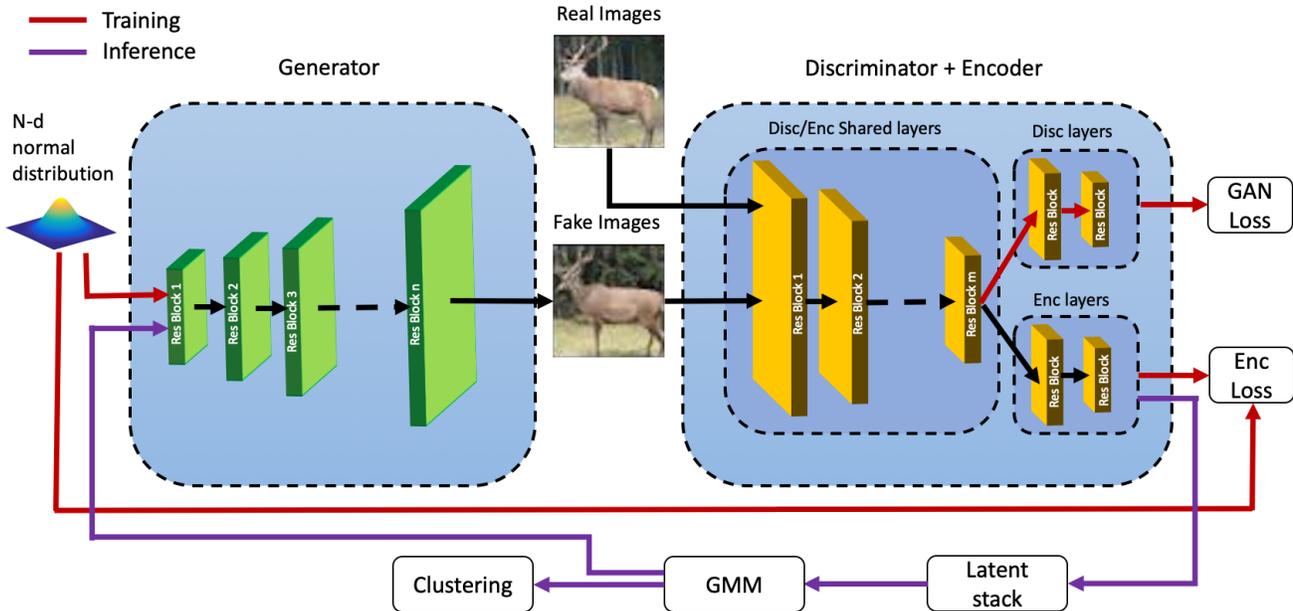


Figure 2: *Our proposed GAEL framework.* GAEL combines the standard GAN architecture with an encoder. The encoder and discriminator train simultaneously, sharing weights except for the last layers. There are two losses: regular GAN loss and the encoder’s own loss. After the training finishes, we aggregate the latent space of the images and model the latent space with a GMM. Then the GMM distribution serves two purposes: 1) for clustering and 2) as an input distribution to the generator.

codes of the images for clustering.

While most GAN works do not provide such capability, several works have explored such directions. Since we propose such a modification to GANs, and show an improvement by doing so, we focus now on works that suggested similar modifications to GAN architectures and are the closest to our work.

ALI [15] suggested using another network for encoding and trained their framework such that it would jointly generate the images and the latent space. It learns to match the joint distribution of the real images with their encoded images, and the generated latent space along with the generated images. To improve the ALI approach, ALICE [38] added a cycle consistent criteria, which used an encoder-generator mechanism to introduce a conditional entropy loss function between the real images and the reconstructed images.

Notice that these works optimize the encoder in a way that enforces its output to have a normal distribution, which is less suited for clustering. In addition, trying to enforce a normal distribution of an output imposes a constraint upon the generator’s ability to generate high quality images. The architecture is also more difficult to train, as the discriminator trains adversarially with not only the generator but also the encoder. This adds complexity to the already complex

training mechanism of GANs. In our work, we propose an alternative path and do not enforce the distribution of the output of the encoder to be similar to the output of the latent distribution. Indeed, we require similarity between the two but in a weaker way. After that, we model the latent distribution with a GMM, which is very different than the actual (normal) distribution used in the training.

InfoGAN [10] maximized the mutual information between the latent space and the generated images. InfoGAN’s results suggest that the network had learned interpretable latent representation. While InfoGAN enforces consistency on only a subspace of the latent space, our approach enforced consistency on the entire latent space. Learning the entire latent space reconstruction gave us the benefit of having an autoencoder. Furthermore, InfoGAN enforces the consistency between the input of the generator and the output of the discriminator through parametric optimization of both networks. Employing such simultaneous matching on both networks prevented the encoder from learning a good representation. This is because the flexibility of training both the generator and discriminator to minimize mutual information may lead to a trivial solution, e.g., encoding everything in one pixel.

VEEGAN [53] takes a different approach. It has two

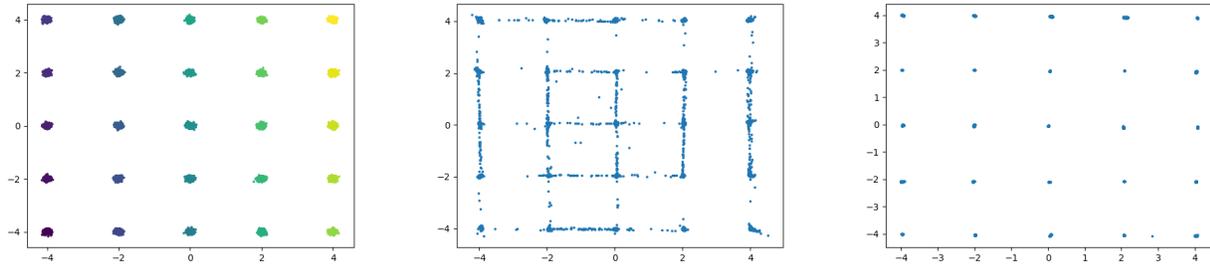


Figure 3: From left to right: Original 5 X 5 toy dataset; WGAN-baseline generated data; and GAEL generated data. Note that while WGAN struggles to learn the data distribution, GAEL uses the exact same architecture but with the addition of an encoder and GMM-modeling of the latent code generates the data much better.

loss terms, one that tries to learn the inverse function of the generator back to the latent space, and a second that tries to minimize the cross entropy between the mapped real images and the prior latent space. VEEGAN enforces consistency across the entire latent space in the output of the encoder ($E(G(z)) - z$), minimizing the network parameters of both the encoder and generator. Minimizing the encoder and generator together leads to the same issues that we described in InfoGAN. VEEGAN also enforces similarity between the original latent space and the output of the encoder’s distribution, because it reduces the entropy between the original latent space and the output of the encoder. As with ALI, a loss function constrains the latent space, which hinders clustering and reduces the quality of the generated images.

Our proposed framework relies also on using Gaussian Mixture Models (GMM) for the GAN latent space. Several previous approaches used mixtures with GANs. The work in [63] suggested using a GAN mixture for clustering. Another work compared GMM performance to the one of GANs for data modeling [51]. PacGAN [40] provides the discriminator with multiple generated examples instead of one to improve the generated diversity and avoid mode collapse. A concurrent strategy [17] provides a novel GAN training that is based on the optimal transport theory for learning Gaussian mixture models. Another approach uses GMM for the input latent space of the GAN [3] and uses it in training. Our method, on the other hand, employs a standard Gaussian distribution during the training. Only at the end do we model the latent distribution as a GMM, using the entire dataset. We sample from the GMM only during inference.

3. The GAEL method

Our method uses a hybrid-architecture, combining a GAN with an encoder network. We call our method Generative Adversarial Encoder Learning (GAEL). We outline our design in Figure 2. It uses a standard generator and discriminator that can be trained with any existing GAN technique. This makes our proposed strategy very generic. To the discriminator, we add an encoder head that shares the same first layers of the discriminator. The goal of the encoder head is to create a latent code for the discriminator’s input images. It is trained using only the fake images with a loss that requires the encoder’s code to match the latent code used in the generator. After the training finishes, we use a new latent distribution, namely, a mixture of Gaussians, as input to the generator. To learn this distribution, we adapt a GMM to all the latent codes generated by the encoder for the data. We also use this GMM to cluster the data.

Our proposed architecture has multiple benefits. The encoder network enables us, naturally, to encode and decode images. Additionally, because it transfers the image space to feature space, the network provides a suitable output for clustering. We also try to use the encoder network to improve the generator’s input distribution. By learning the real images’ latent space distribution, we can replace the normal distribution with the new learned distribution.

To summarize, we test GAEL on three separate tasks: (i) autoencoding; (ii) generation; and (iii) clustering. We turn now to describe each part of our proposed framework and its utility in these tasks.

The encoder. The generator G maps each sample $Z \in R^M$ from the latent space to an image $X \in R^{N \times N}$ in the image space, i.e., $x = G(z)$. While we can find the corresponding x for each z using G , the inverse is not always possible as G is not necessarily invert-

	CIFAR10		CIFAR100		STL10 (48x48)	
	IS	FID	IS	FID	IS	FID
WGAN-GP [21]	7.86	-	-	-	-	-
CT-GAN [59]	8.12	-	-	-	-	-
SN-GAN [44]	8.22	21.7	-	-	9.1	40.1
AutoGAN [19]	8.55	12.42	-	-	9.16	31.01
progressive GAN [33]	8.8	10.7	-	-	-	-
E ² GAN [54]	8.51	11.26	-	-	9.51	25.35
Baseline WGAN	8.49	12.89	8.62	17.37	9.09	40.71
Baseline+Encoder WGAN(our)	8.76	8.76	8.86	13.42	10.00	27.44
GMM-10 WGAN(our)	9.15	7.70	9.26	13.98	10.39	23.39
GMM-50 WGAN(our)	9.24	7.83	9.46	12.96	10.75	22.57
BigGAN [6] (supervised)	9.22	14.73	-	-	-	-
MHingeGAN [35] (supervised)	9.58	7.5	14.36	17.3	12.16	17.59

Table 1: GAN inception score and FID of our method compared to some baselines on three datasets; best results are highlight in **bold**. We present existing supervised GAN results only for reference. Notice that our GAN is unsupervised but achieves improved results compared to the BigGAN whose GAN architecture and loss are very similar to ours.

ible. To alleviate that, we train an encoder that learns the inverse function using probabilistic regression. We choose the following likelihood for the inverse function:

$$P(z|x) \sim N(Enc(x), \Sigma(x)), \quad (1)$$

where $Enc(x)$ is the first encoder output, which estimates the latent vector that generated the input x , and $\Sigma(x)$ is another encoder output that serves as confidence or variance of the estimation of $Enc(x)$. The goal of the confidence output is twofold: (i) as mentioned above, having a strict condition in the training on the relationship between the generating latent code and the output of the encoder may harm training. The variance helps to mitigate this issue; (ii) this confidence might be useful in some tasks, e.g., using it as a weight in clustering (we do not use it in this work but this is a possibility for future work).

Our encoder shares most of its weights with the discriminator, with only the last few layers being independent. This helps the encoder learn meaningful features, while adding very little to the training time. The encoder loss is the log likelihood of Equation (1):

$$\log(P(z|x)) = -0.5 \log(((2\pi)^M |\Sigma(x)|)) - 0.5(z - Enc(x))^T \Sigma^{-1}(x) (z - Enc(x)). \quad (2)$$

We also tried to enforce "consistency loss." We attempted this by passing the original images through an encoder-generator-encoder sequence, and asked for consistency between the first encoded images and the last ones. I.e., adding $\min(E(G(E(X))) - E(X))$. We tried variations of this set up: e.g. freezing the generator and training the encoder; freezing the encoder while

training the generator; and freezing neither, and training both concurrently. All cases led to heavy degradation across all categories of network performance. The failure of this consistency loss led us to the idea that the encoder's training should interfere with GAN training as little as possible. Our current setup allows this. Moreover, in our framework, the ability to use the encoder to reconstruct images does not compromise image generation quality but rather strengthens it.

GAEL loss function. As the encoder is trained with the GAN as a whole, we combine encoder and GAN loss. There are many varieties of the loss function for GAN. For the presentation simplicity, we explain our method on the loss function below. However, it can work on other loss functions as well (as we show in the experiments, where we use our loss also with the Wasserstein GAN).

$$\min_G \max_D V(D, G) = E_{x \sim P_{data}} [\log D(x)] + E_{z \sim noise} [\log(1 - D(G(z)))]. \quad (3)$$

This leads to the following loss function that is used for GAEL training:

$$\min_G \max_{D, Enc, \sigma} V(D, G) + \lambda E_{x, z \sim P(x, z)} [\log(P(z|x))], \quad (4)$$

where λ is a hyperparameter that balances the weight of the encoder in the training. We set its value to 10 in all experiments (the network performed similarly when we tried other values for λ as well).

Clearly, we can plug our Encoder with its loss in any other GAN framework just by replacing $V(D, G)$

with the appropriate loss. For example, if we used the WGAN loss, then the encoder would share weights with the critic (WGAN’s alternative to the discriminator).

Autoencoder. To use GAEL as an autoencoder, we simply calculate the encoding of the input image x using $Enc(x)$. Then we reconstruct the image using the (trained) generator G , which serves as the decoder in this case.

Generation. When we train the GAN, we use inputs that are drawn from a random Gaussian distribution. Thus, a straightforward way to generate new data with the generator is to draw random vectors from the same distribution and use them to generate new examples using G .

One of the drawbacks of GANs is that some of their outputs do not really belong to the true distribution. Therefore, we want to avoid these regions in the original latent distribution that leads to such outputs. To do so, we attempt to model the latent distribution of the original images by a parametric distribution. Specifically, we use GMM. To do that, we pass all the (true) data through the encoder to get a feature space for each image. We then fit a GMM to the encoded features. Having this GMM, we can sample a latent vector from it, which is then used for input to the generator.

While other distributions could have been used, our focus in this work is on images. Images have a high degree of variability (e.g., different features and semantic content). To capture the multiple modalities of this data, we use a multi-modal distribution, the GMM.

Clustering. GMM typically works well for clustering when the images within the clusters are in close Euclidean space (e.g., MNIST), but struggles to cluster images of highly varied semantic information [61]. To achieve better results while working with complex data, meaningful representation needs to be learned. Here is where deep learned features can be used [1, 42]. In particular to our case, GAEL may use a GMM on the latent distribution generated by the encoder from the real data in order to cluster.

If the encoder learns meaningful representation, i.e., keeps similar semantic images together in the latent space, then the clustering can be done with traditional clustering algorithms (e.g., Kmeans and GMMs) on the latent space of the original images. As mentioned above, we use GMM. We calculate a GMM for the whole data and then assign each input image to the Gaussian that has its largest probability.

Toy Example. We use a simple toy example to demonstrate our method. Figure 3(left) shows the original toy dataset, a GMM distribution with 25 components spread in a two-dimensional grid pattern. On this

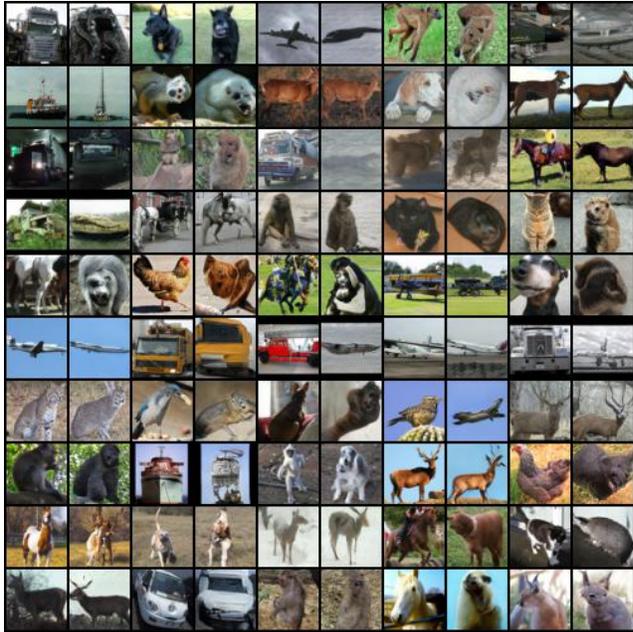


Figure 4: Encoder-generator image reconstruction. Even columns contain the original images, odd contain reconstructions.

toy dataset, we trained a baseline Wasserstein GAN and GAEL (i.e. the same GAN but with the addition of the encoder). Figure 3(middle) shows the results of the baseline generator. While it succeeded to recreate the original modes, it also left artifacts between them. These artifacts are hard to remove. We suggest this difficulty may owe to the fact that GAN architecture struggles to convert a smooth, i.e. normal, distribution to such a mode-disjoint one.

On the contrary, our method uses a GMM-distribution for our latent space, which is multi-modal and thus likely to be more adequate to the input latent distribution. Figure 3(right) exhibits our method. Note that in this case, the generated data matches the locations of the original data. More details on this experiment appear in the sup. material.

4. Experiments

Except for STL-10, we used the BigGAN [6] architecture for all datasets, with minimal modification. For the STL-10 dataset, we employ MHGAN [35]. We also applied the same hyper-parameters throughout the experiments. We tested our method’s performance on three different applications: image generation, image reconstruction, and clustering.

Our experiments use the following data sets to train and evaluate our method: CIFAR-10, CIFAR-100,

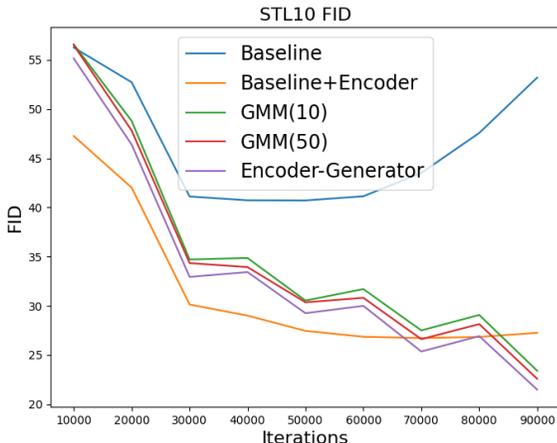


Figure 5: FID score across iterations trained on the STL-10 dataset. The baseline network performance degrades considerably as training progresses. Adding our encoder not only improves the scores, but also dramatically reduces this performance degradation. Incorporating the GMM further improves performance and stabilizes the training procedure. The encoder-generator network constitutes an upper bound for the GAEL performance.

STL-10, CelebA, MNIST and ImageNet. We present here quantitative results for the first three datasets on the clustering and image generation tasks. We also show some visual results in the paper, but more is covered in the supplementary material, which presents all the datasets.

We model the $\Sigma(x)$ by diagonal matrix. During our experiments, we found that learning the $\Sigma(x)$ lead to similar results as using $\Sigma(x) = I$, which made our method even simpler.

4.1. Image reconstruction

Our first experiment tests the visual quality of our encoder-generator reconstruction of the original images. This test was done by encoding the original images and reconstructing them with the generator. We then compare the originals with the reconstructions to evaluate whether our encoder had learned meaningful representation. We present the original and reconstructed images side-by-side in Figure 4. More examples on all datasets appear in the supplementary material.

The figures show that the network was able to reconstruct images with similar semantic information and with high quality. Note though that it does not reconstruct the same input image. This is a desirable

property. We want to keep the same semantics, as we want the encodings to be useful for clustering. Yet, we do not want to have a strict tie between the input of the generator and the code of the encoder. We found that adding such a strict constraint in training degrades the performance of the generated images significantly, as it limits the generator flexibility. This might be the reason for the lower image quality that was achieved in previous works that tried to have exact matches in the encoding. We are not aware of a previous work that is able to achieve the quality of reconstruction that we achieved here, with a generator that contains an encoder (see the results on STL-10 and ImageNet, particularly challenging datasets).

4.2. Image generation

Our second experiment tested how well our network generated images. To measure generation quality, we used the inception [52] and FID [25] scores. For both metrics, we used the author’s original code.

Table 1 presents scores for our baseline, essentially a modified version of the BigGAN code with the projection discriminator removed. We established our GAEL architecture by adding the encoder to this model. Our results demonstrate that we achieve significant improvement upon this baseline by adding our encoder and its loss function. This implies that our encoder is not only capable of encoding images (as demonstrated in Section 4.1), but also improves GAN performance. We show the results with and without the GMM encoding of the latent space.

Notice that we get improvement even before adding the GMM. We also show the impact of the number of Gaussians in the GMM on the performance.

In the supplementary material, we show the generation results of GAEL based on vanilla GAN. Again, adding the encoder gives a significant boost in performance, which is further improved with the GMM-modeling of the latent space. This demonstrates that our method is generic and can be used with a variety of GANs and is not restricted to a specific GAN model.

In Table 1, we compare GAEL to other methods. We may divide these methods into two groups: the first, which does not use the labels included in the data set (unsupervised), and the second, which does use the data set labels(supervised). Clearly, having the labels provides a big advantage. Yet, using GAEL with GMM, we get better results than the BigGAN, which has our architecture, but uses labels. We also come very close to the results of the strong supervised technique, MHingeGAN [35]. This shows the power of our approach, which does not use any labels during training but rather models the latent space via a

	CIFAR10			CIFAR100			STL10		
	NMI	ARI	ACC	NMI	ARI	ACC	NMI	ARI	ACC
GAN [50]	0.265	0.176	0.315	0.120	0.045	0.151	0.2100	0.139	0.298
JULE [62]	0.192	0.138	0.271	0.103	0.033	0.137	0.182	0.164	0.277
DEC [60]	0.257	0.161	0.301	0.136	0.049	0.185	0.276	0.186	0.359
TUM [23]	-	-	0.325	-	-	-	-	-	0.530
DAC [8]	0.396	0.306	0.522	0.185	0.088	0.238	0.366	0.257	0.470
ClusterGAN[48]	0.323	-	0.412	-	-	-	0.335	-	0.423
Our	0.443	0.350	0.555	0.289	0.135	0.299	0.377	0.230	0.383

Table 2: Clustering results of various method on three datasets, best results highlight in **bold**

GMM. Notice also our advantage over other unsupervised approaches.

Note that BigGAN applies a "truncation trick" [6], which truncates the normal distribution in order to achieve improved FID and Inception scores. This trick and the GMM modeling come from the same core idea—improving the latent space. However, while BigGAN uses a trick to achieve this, including a truncation threshold hyper-parameter, our approach is more fundamental and based on direct learning from the data.

To establish an upper bound of GAEL’s ability to generate images, we measured the FID and inception scores on the reconstructions themselves. Because we generated these images from our encoded original images, we cannot of course compare these specific results with independent methods. However, these scores provided us an upper bound of what our encoder could achieve, and therefore provided a target that the network could aim at when generating images. We call this approach Encoder-Generator.

We found that the encoder introduced stability to the training procedure. We measured the FID and IS scores of generated images across all iterations of the GAN, trained with and without the encoder. Figure 5 shows the FID results for STL-10. More examples appear in the supplementary material. While the scores of the network without the encoder degraded substantially as training progressed, GAEL experienced almost no loss at all. Note that the addition of the encoder greatly stabilized training and that the results of GAEL with GMM are not far from the results of the upper bound Encoder-Generator.

4.3. Clustering

Our final experiment tested our method’s ability to cluster. To evaluate our clustering, we fit the GMM to the latent space, this time with the number of mixture models being equal to the number of labels in each dataset. Then each image was assigned to one of the mixture models. We evaluated the performance

of our clustering algorithm using the Adjusted Rand Index (ARI), Normalized Mutual Information (NMI), and clustering Accuracy (ACC). A qualitative demonstration of our clustering can be found in the supplementary materials.

Table 2 shows that our results exceed the performance obtained by all other GAN-based clustering. On the CIFAR-10 and CIFAR-100 benchmarks, GAEL’s performance, as measured by all metrics, delivers the best results compared to all methods. On the STL-10 dataset, two CNN-based (not GAN-based) approaches, TUM and DAC, outperform our clustering results.

5. Conclusion

This paper presents GAEL, a simple and effective approach to enhancing GAN performance by incorporating an encoder into its architecture. GAEL’s simplicity derives from its low number of variables and simple loss function, which has only one hyperparameter. GAEL works robustly for a wide range of values of this parameter. Additionally, our encoder can be incorporated into almost any GAN architecture with negligible computational or training time cost. Beyond its performance improvements, it also adds a secondary benefit of stabilizing the training procedure.

Our results exhibit the encoder’s utility in three separate applications: image reconstruction, generation, and clustering. We tested the architecture on a variety of different datasets using both metrical and qualitative analysis. In all cases, GAEL achieved high performance. We also tried to continue training GAEL with the new latent space of the GMM. This showed a small improvement, which was not significant enough to be presented here. Yet, a more sophisticated training could have benefited from this combination and we defer this to a future study. Another interesting direction is adapting our technique to the tasks of semi-supervised and few-shot learning. We hope that our proposed methodology will be found beneficial for many other applications and for improving other ap-

proaches to GAN.

Acknowledgement We would like to thank Matt Dodson, for his writing advice and editorial oversight.

References

- [1] Elie Aljalbout, Vladimir Golkov, Yawar Siddiqui, and Daniel Cremers. Clustering with deep learning: Taxonomy and new methods. *CoRR*, abs/1801.07648, 2018. [6](#)
- [2] Martín Arjovsky, Soumith Chintala, and Léon Bottou. Wasserstein generative adversarial networks. In *ICML*, 2017. [2](#)
- [3] Matan Ben-Yosef and Daphna Weinshall. Gaussian mixture generative adversarial networks for diverse datasets, and the unsupervised clustering of images, 2018. [4](#)
- [4] David Berthelot, Tom Schumm, and Luke Metz. Began: Boundary equilibrium generative adversarial networks. *arXiv preprint arXiv:1703.10717*, 2017. [2](#)
- [5] Piotr Bojanowski, Armand Joulin, David Lopez-Pas, and Arthur Szlam. Optimizing the latent space of generative networks. In *International Conference on Machine Learning*, pages 599–608, 2018. [2](#)
- [6] Andrew Brock, Jeff Donahue, and Karen Simonyan. Large scale gan training for high fidelity natural image synthesis. *CoRR*, abs/1809.11096, 2019. [1](#), [5](#), [6](#), [8](#)
- [7] Eoin Brophy, Zhengwei Wang, and Tomas E. Ward. Quick and easy time series generation with established image-based gans. *ArXiv*, abs/1902.05624, 2019. [1](#)
- [8] Jianlong Chang, Lingfeng Wang, Gaofeng Meng, Shiming Xiang, and Chunhong Pan. Deep adaptive image clustering. In *Proceedings of the IEEE Conference on Computer Vision and Pattern Recognition*, pp. 5879–5887, 2017. [8](#)
- [9] Ting Chen, Xiaohua Zhai, Marvin Ritter, Mario Lucic, and Neil Houlsby. Self-Supervised GANs via Auxiliary Rotation Loss. *2019 IEEE/CVF Conference on Computer Vision and Pattern Recognition (CVPR)*, pages 12146–12155, 2019. [2](#)
- [10] Xi Chen, Yan Duan, Rein Houthoofd, John Schulman, Ilya Sutskever, and Pieter Abbeel. Infogan: Interpretable representation learning by information maximizing generative adversarial nets. In *NIPS*, 2016. [3](#)
- [11] Emily L Denton, Soumith Chintala, Arthur Szlam, and Robert Fergus. Deep Generative Image Models using a Laplacian Pyramid of Adversarial Networks. *CoRR*, abs/1506.0, 2015. [2](#)
- [12] Jeff Donahue, Philipp Krähenbühl, and Trevor Darrell. Adversarial feature learning. *ICLR*, 2017. [2](#)
- [13] Jeff Donahue and Karen Simonyan. Large scale adversarial representation learning, 2019. [2](#)
- [14] Sivan Dovel and Raja Giryes. Degas: Differentiable efficient generator search, 2019. [2](#)
- [15] Vincent Dumoulin, Ishmael Belghazi, Ben Poole, Alex Lamb, Martin Arjovsky, Olivier Mastropietro, and Aaron Courville. Adversarially learned inference. *arXiv:1606.00704*, 2016. [3](#)
- [16] Gintare Karolina Dziugaite, Daniel M. Roy, and Zoubin Ghahramani. Training generative neural networks via maximum mean discrepancy optimization. *ArXiv*, abs/1505.03906, 2015. [1](#)
- [17] Farzan Farnia, William Wang, Subhro Das, and Ali Jadbabaie. Gat-gmm: Generative adversarial training for gaussian mixture models, 2020. [4](#)
- [18] William Fedus, Ian Goodfellow, and Andrew M. Dai. MaskGAN: Better text generation via filling in the .. In *International Conference on Learning Representations*, 2018. [1](#)
- [19] Xinyu Gong, Shiyu Chang, Yifan Jiang, and Zhangyang Wang. Autogan: Neural architecture search for generative adversarial networks. In *Proceedings of the IEEE/CVF International Conference on Computer Vision (ICCV)*, October 2019. [2](#), [5](#)
- [20] Ian Goodfellow, Jean Pouget-Abadie, Mehdi Mirza, Bing Xu, David Warde-Farley, Sherjil Ozair, Aaron Courville, and Yoshua Bengio. Generative adversarial nets. In *Advances in neural information processing systems*, pages 2672–2680, 2014. [2](#)
- [21] Ishaan Gulrajani, Faruk Ahmed, Martin Arjovsky, Vincent Dumoulin, and Aaron C Courville. Improved training of wasserstein gans. In *Advances in Neural Information Processing Systems*, volume 30, pages 5767–5777, 2017. [2](#), [5](#)
- [22] Jiaxian Guo, Sidi Lu, Han Cai, Weinan Zhang, Yong Yu, and Jun Wang. Long text generation via adversarial training with leaked information. In Sheila A. McIlraith and Kilian Q. Weinberger, editors, *Proceedings of the Thirty-Second AAAI Conference on Artificial Intelligence, (AAAI-18), the 30th innovative Applications of Artificial Intelligence (IAAI-18), and the 8th AAAI Symposium on Educational Advances in Artificial Intelligence (EAAI-18), New Orleans, Louisiana, USA, February 2-7, 2018*, pages 5141–5148. AAAI Press, 2018. [1](#)
- [23] Philip Haeusser, Johannes Plapp, Vladimir Golkov, Elie Aljalbout, and Daniel Cremers. Associative deep clustering: Training a classification network with no labels. In *Proceedings of the German Conference on Pattern (GCPR)*, 2018. [8](#)
- [24] Kay Gregor Hartmann, Robin Tibor Schirrmeyer, and Tonio Ball. Eeg-gan: Generative adversarial networks for electroencephalographic (eeg) brain signals. *ArXiv*, abs/1806.01875, 2018. [1](#)
- [25] Martin Heusel, Hubert Ramsauer, Thomas Unterthiner, Bernhard Nessler, and Sepp Hochreiter. Gans trained by a two time-scale update rule converge to a local nash equilibrium. In *NIPS*, 2017. [2](#), [7](#)
- [26] Yedid Hoshen and Lior Wolf. Nam: Non-adversarial unsupervised domain mapping. In *ECCV*, pages 455–470, 2018. [2](#)
- [27] Shady Abu Hussein, Tom Tirer, and Raja Giryes. Image-adaptive gan based reconstruction, 2019. [1](#)

- [28] Phillip Isola, Jun-Yan Zhu, Tinghui Zhou, and Alexei A. Efros. Image-to-image translation with conditional adversarial networks. *2017 IEEE Conference on Computer Vision and Pattern Recognition (CVPR)*, pages 5967–5976, 2016. 1
- [29] Nikolay Jetchev, Urs Bergmann, and Roland Vollgraf. Texture synthesis with spatial generative adversarial networks. *CoRR*, abs/1611.08207, 2016. 1
- [30] Takuhiro Kaneko, Kaoru Hiramatsu, and Kunio Kashino. Generative attribute controller with conditional filtered generative adversarial networks. *2017 IEEE Conference on Computer Vision and Pattern Recognition (CVPR)*, pages 7006–7015, 2017. 2
- [31] Tero Karras, Timo Aila, Samuli Laine, and Jaakko Lehtinen. Progressive Growing of GANs for Improved Quality, Stability, and Variation. *CoRR*, abs/1710.1, 2017. 2
- [32] Tero Karras, Timo Aila, Samuli Laine, and Jaakko Lehtinen. Progressive Growing of {GAN}s for Improved Quality, Stability, and Variation. In *International Conference on Learning Representations*, 2018. 1
- [33] Tero Karras, Timo Aila, Samuli Laine, and Jaakko Lehtinen. Progressive growing of GANs for improved quality, stability, and variation. In *International Conference on Learning Representations*, 2018. 5
- [34] Tero Karras, Samuli Laine, and Timo Aila. A Style-Based Generator Architecture for Generative Adversarial Networks. *2019 IEEE/CVF Conference on Computer Vision and Pattern Recognition (CVPR)*, pages 4396–4405, 2019. 2
- [35] Ilya Kavalerov, Wojciech Czaja, and Rama Chellappa. A multi-class hinge loss for conditional gans. In *Proceedings of the IEEE/CVF Winter Conference on Applications of Computer Vision (WACV)*, January 2021. 5, 6, 7
- [36] Diederik P Kingma and Max Welling. Auto-encoding variational bayes, 2013. 2
- [37] Christian Ledig, Lucas Theis, Ferenc Huszár, José Antonio Caballero, Andrew Aitken, Alykhan Tejani, Johannes Totz, Zehan Wang, and Wenzhe Shi. Photo-Realistic Single Image Super-Resolution Using a Generative Adversarial Network. *2017 IEEE Conference on Computer Vision and Pattern Recognition (CVPR)*, pages 105–114, 2017. 1
- [38] Chunyuan Li, Hao Liu, Changyou Chen, Yuchen Pu, Liqun Chen, Ricardo Henao, and Lawrence Carin. Alice: Towards understanding adversarial learning for joint distribution matching. In I. Guyon, U. V. Luxburg, S. Bengio, H. Wallach, R. Fergus, S. Vishwanathan, and R. Garnett, editors, *Advances in Neural Information Processing Systems*, volume 30, pages 5495–5503. Curran Associates, Inc., 2017. 3
- [39] Chun-Liang Li, Wei-Cheng Chang, Yu Cheng, Yiming Yang, and Barnabas Poczos. Mmd gan: Towards deeper understanding of moment matching network. In *Advances in Neural Information Processing Systems*, volume 30, pages 2203–2213. Curran Associates, Inc., 2017. 2
- [40] Zinan Lin, Ashish Khetan, Giulia C. Fanti, and Seungwon Oh. Pacgan: The power of two samples in generative adversarial networks. In *NeurIPS*, 2018. 4
- [41] Pauline Luc, Camille Couprie, Soumith Chintala, and Jakob Verbeek. Semantic segmentation using adversarial networks. *ArXiv*, abs/1611.08408, 2016. 1
- [42] Erxue Min, Xifeng Guo, Qiang Liu, Gen Zhang, Jianjing Cui, , and Jun Long. A survey of clustering with deep learning: From the perspective of network architecture. *IEEE Access*, 6:39501–39514, abs/1801.07648, 2018. 6
- [43] Mehdi Mirza and Simon Osindero. Conditional generative adversarial nets. *CoRR*, abs/1411.1784, 2014. 2
- [44] Takeru Miyato, Toshiki Kataoka, Masanori Koyama, and Yuichi Yoshida. Spectral normalization for generative adversarial networks. In *International Conference on Learning Representations*, 2018. 2, 5
- [45] Takeru Miyato and Masanori Koyama. cGANs with projection discriminator. In *International Conference on Learning Representations*, 2018. 2
- [46] Yao Ni, Dandan Song, Xi Zhang, Hao Wu, and Lejian Liao. Cagan: Consistent adversarial training enhanced gans. In *International Joint Conference on Artificial Intelligence (IJCAI)*, 2018. 2
- [47] Sung Woo Park and Junseok Kwon. Sphere Generative Adversarial Network Based on Geometric Moment Matching. *2019 IEEE/CVF Conference on Computer Vision and Pattern Recognition (CVPR)*, pages 4287–4296, 2019. 2
- [48] A. Radford, L. Metz, and S. Chintala. Unsupervised representation learning with deep convolutional generative adversarial network. *s. CoRR*, abs/1511.06434, 2015. 8
- [49] Alec Radford, Luke Metz, and Soumith Chintala. Unsupervised Representation Learning with Deep Convolutional Generative Adversarial Networks. *CoRR*, abs/1511.0, 2015. 2
- [50] Alec Radford, Luke Metz, and Soumith Chintala. Unsupervised representation learning with deep convolutional generative adversarial networks. *CoRR*, abs/1511.06434, 2016. 8
- [51] Eitan Richardson and Yair Weiss. On gans and gmms. In *NeurIPS*, 2018. 4
- [52] Tim Salimans, Ian Goodfellow, Wojciech Zaremba, Vicki Cheung, Alec Radford, and Xi Chen. Improved techniques for training gans. In *Advances in Neural Information Processing Systems*, pages 2234–2242, 2016. 2, 7
- [53] A. Srivastava, C. Valkov, L. and Russell, M. Gutmann, and C. Sutton. Veegan: Reducing mode collapse in gans using implicit variational learning. In *Advances in Neural Information Processing Systems*, 2017. 3
- [54] Yuan Tian, Qin Wang, Zhiwu Huang, Wen Li, Dengxin Dai, Minghao Yang, Jun Wang, and Olga Fink. Off-policy reinforcement learning for efficient and effective

- gan architecture search. In *Computer Vision – ECCV 2020*, pages 175–192, 2020. [2](#), [5](#)
- [55] Hanchao Wang and Jun Huan. Agan: Towards automated design of generative adversarial networks, 2019. [2](#)
- [56] T. Wang, M. Liu, J. Zhu, A. Tao, J. Kautz, and B. Catanzaro. High-resolution image synthesis and semantic manipulation with conditional gans. In *2018 IEEE/CVF Conference on Computer Vision and Pattern Recognition*, pages 8798–8807, June 2018. [1](#)
- [57] Ting-Chun Wang, Ming-Yu Liu, Jun-Yan Zhu, Andrew Tao, Jan Kautz, and Bryan Catanzaro. High-resolution image synthesis and semantic manipulation with conditional gans. *IEEE/CVF Conference on Computer Vision and Pattern Recognition*, pages 8798–8807, 2018. [2](#)
- [58] Wei Wang, Yuan Sun, and Saman Halgamuge. Improving MMD-GAN training with repulsive loss function. In *International Conference on Learning Representations*, 2019. [2](#)
- [59] Xiang Wei, Boqing Gong, Zixia Liu, Wei Lu, and Liqiang Wang. Improving the improved training of wasserstein gans. *ICLR*, 2018. [2](#), [5](#)
- [60] J. Xie, R. Girshick, and A. Farhadi. Unsupervised deep embedding for clustering analysis. In *ICML*, pages 478–48, 2016. [8](#)
- [61] Dongkuan Xu and Yingjie Tian. A comprehensive survey of clustering algorithms. *Annals of Data Science*, 2(2):165–193, Jun 2015. [2](#), [6](#)
- [62] J. Yang, D. Parikh, and D. Batra. Joint unsupervised learning of deep representations and image clusters. In *CVPR*, pages 5147–5156, 2016. [8](#)
- [63] Yang Yu and Wen-Ji Zhou. Mixture of gans for clustering. In *Proceedings of the Twenty-Seventh International Joint Conference on Artificial Intelligence, IJCAI-18*, pages 3047–3053. International Joint Conferences on Artificial Intelligence Organization, 7 2018. [4](#)
- [64] Han Zhang, Ian J Goodfellow, Dimitris N Metaxas, and Augustus Odena. Self-Attention Generative Adversarial Networks. *ArXiv*, abs/1805.0, 2019. [2](#)

GMM-Based Generative Adversarial Encoder Learning Supplementary Material

Yuri Feigin, Hedva Spitzer and Raja Giryes
School of Electrical Engineering
Tel Aviv University
Israel, 69978
yurifeigin@mail,raja@tauex.tau.ac.il

Abstract

Here we present some additional examples for the main paper.

1. Toy example

A toy example may provide the reader some intuition about how our method functions. As this demonstration is on paper, here we use a two-dimensional latent space in scatter grid. We projected both the original samples (figure 1a) and the generated images (from a normal distribution) (figure 1b) into two-dimensional space (figures 1c and 1d, respectively). Comparing the two latent spaces, we find that, while the main modes are represented fairly clearly, there is also evidence of object mixing in the latent space, as indicated by the artefacts between the modes. Modelling the latent space of the original samples with the GMM reduces these artefacts, as we discussed in the paper.

The reader may also note that this new latent space is not distributed normally, because there are many regions between the modes without any density.

2. Image reconstruction

In figures 2, 5, 8, 11, 14, 16, we show more results of image reconstruction on the datasets MNIST, CIFAR10, CIFAR100, STL10, CelebA, and Imagenet. We used relative small batch size of 256 images to train the Imagenet.

For all datasets, the images reconstructed well, retaining the originals' semantic information. However the Imagenet results are more mixed. Although the network seemed to handle certain objects well (e.g. dogs, buildings, and cars), it struggled to handle other classes. Despite admitted imperfections, we think the results are promising.

While our attempts with ALI struggled with MNIST, GAEL seems to have handled the dataset well.

3. Image generation

This section presents GAEL's image generation results compared to two baselines, WGAN and Vanilla GAN.

3.1. WGAN (as in main paper)

In figures 3, 4, 6, 7, 9, 10, 12, 13, 15, 17, we present the image generation performances of the baseline WGAN and GAEL. We invite the reader to compare their results on each dataset. Because we trained our Imagenet Dataset on a resolution of 64 x 64, we do not have a reference to compare the results there to any other methods. Nonetheless we wish to summarize the results here. The baseline IS and FID scores were 13.14 and 33.03, respectively. For the baseline with encoder loss, the results were 14.60 and 20.42. Lastly, the results of the GMM were 14.78 and 22.66. We can see that GAEL improved the results over the baseline.

3.2. Vanilla GAN

Table 1 compares our results with a baseline, *Vanilla GAN* whose architecture was based on BigGAN and which used the original GAN loss. The other rows show our method's progressive modifications upon Vanilla GAN. First, by adding an encoder, then by fitting GMMs of ten and fifty. On each data set, our method consistently improved the results of the baseline. While on the CIFAR10 and CIFAR100 datasets, the GMM-50/Encoder combination yielded the best results, for the STL-10 data set, the encoder GAN (without the GMM) fared better. A possible explanation lies in the varied nature of the STL-10 dataset. If the Vanilla GAN struggled to generate images on it, then the encoder would not work well either.

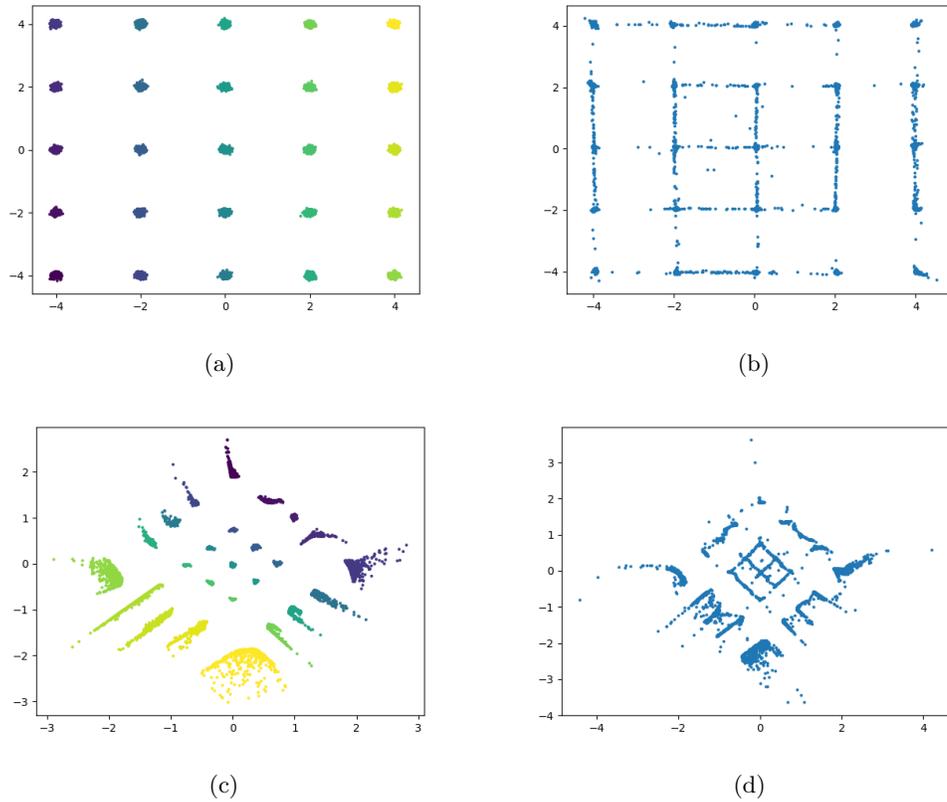


Figure 1: Top left shows the original 5 x 5 toy dataset. Bottom left, the encoded original dataset. Top right, the WGAN baseline generated data. Bottom right, the encoded generated data.

	CIFAR10		CIFAR100		STL10 (48x48)	
	IS	FID	IS	FID	IS	FID
Baseline Vanilla GAN	7.68	34.23	7.75	39.1	6.57	66.93
Baseline+Encoder Vanilla GAN(our)	7.33	28.51	6.97	33.19	8.04	43.64
GMM-10 Vanilla GAN(our)	8.20	20.64	7.98	28.26	7.48	55.80
GMM-50 Vanilla GAN(our)	8.24	20.16	8.00	27.98	7.72	54.39

Table 1: Vanilla GAN inception score and FID of our method compared to some baselines on three datasets; best results are highlighted in **bold**.

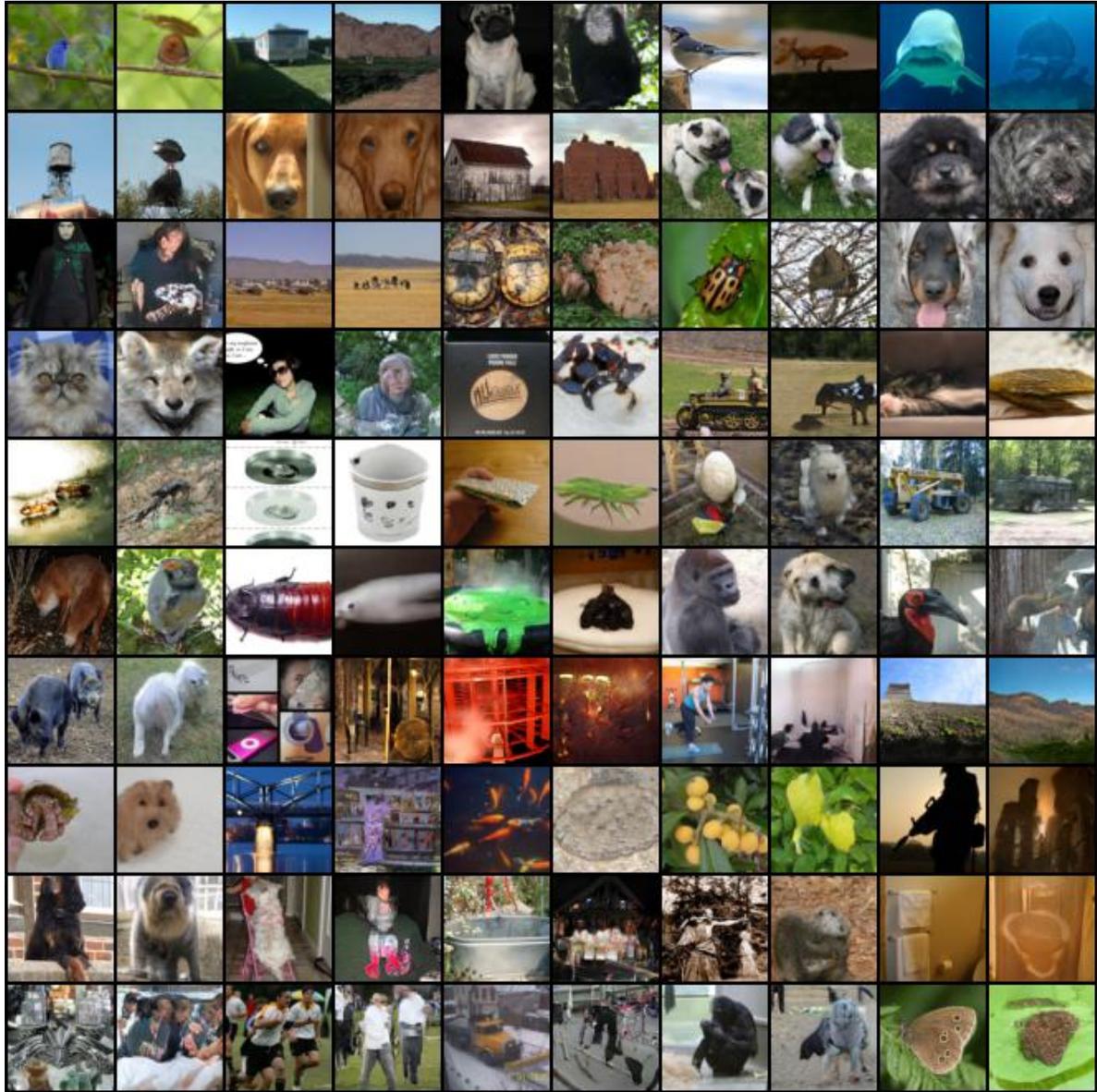


Figure 2: Encoder-generator Imagenet 64x64 image reconstruction. Even columns contain the original images, odd contain reconstructions. Random sample.

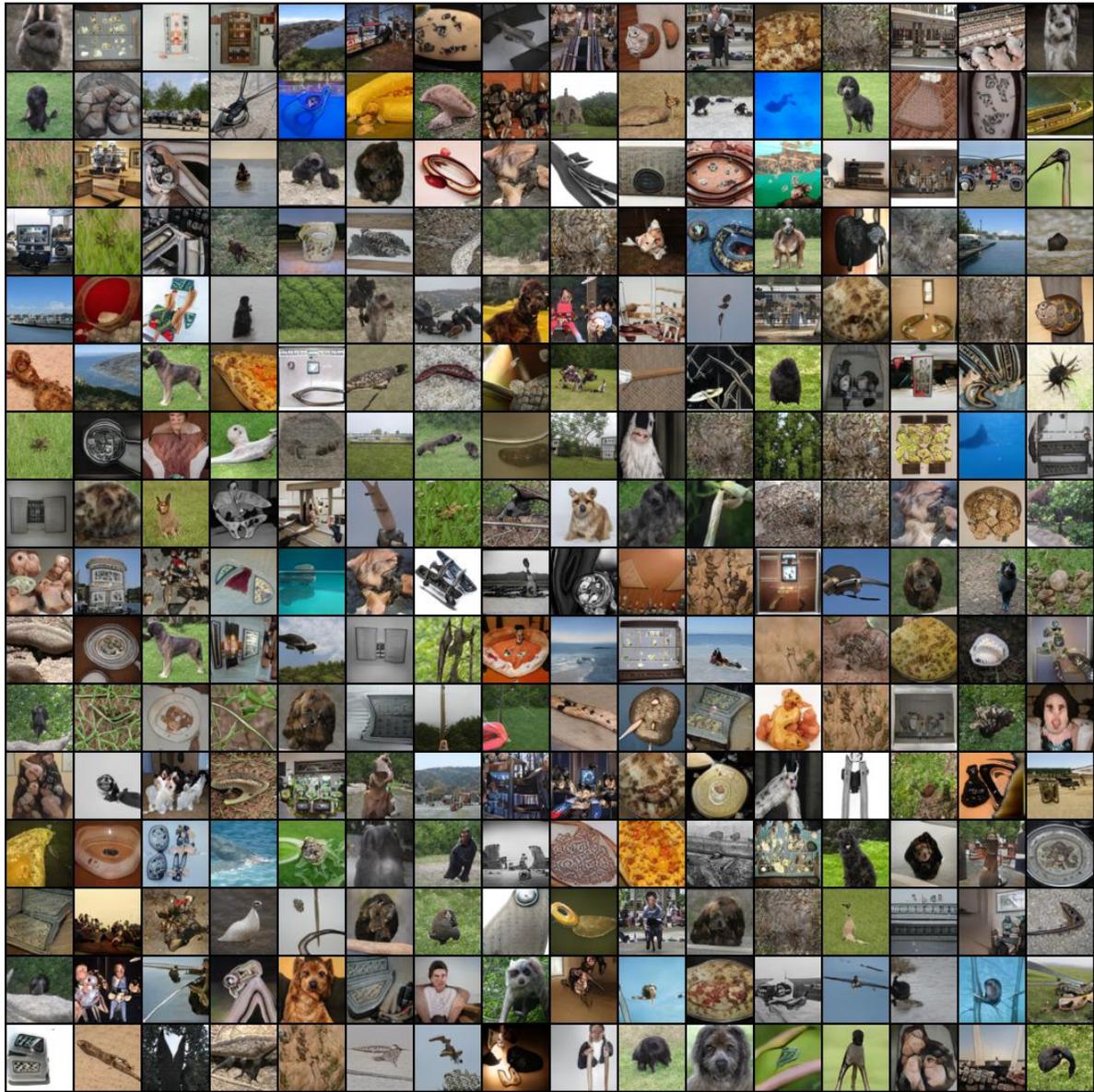


Figure 3: Imagenet 64x64 image generation with baseline. Randomly sampled. Compare to Figure 4.

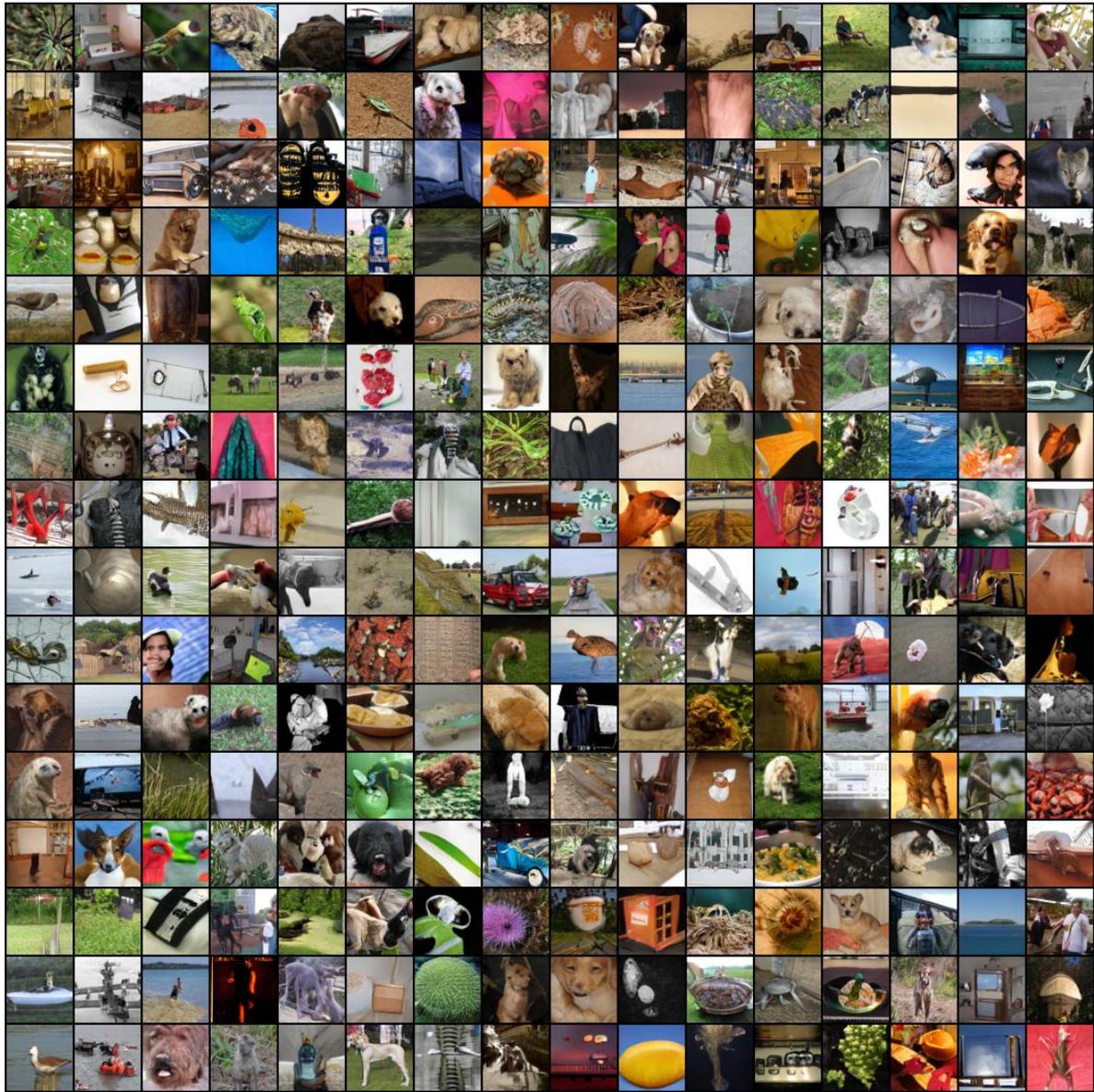


Figure 4: Imagenet 64x64 image generation with GAEL. Randomly sampled. Compare to Figure 3.

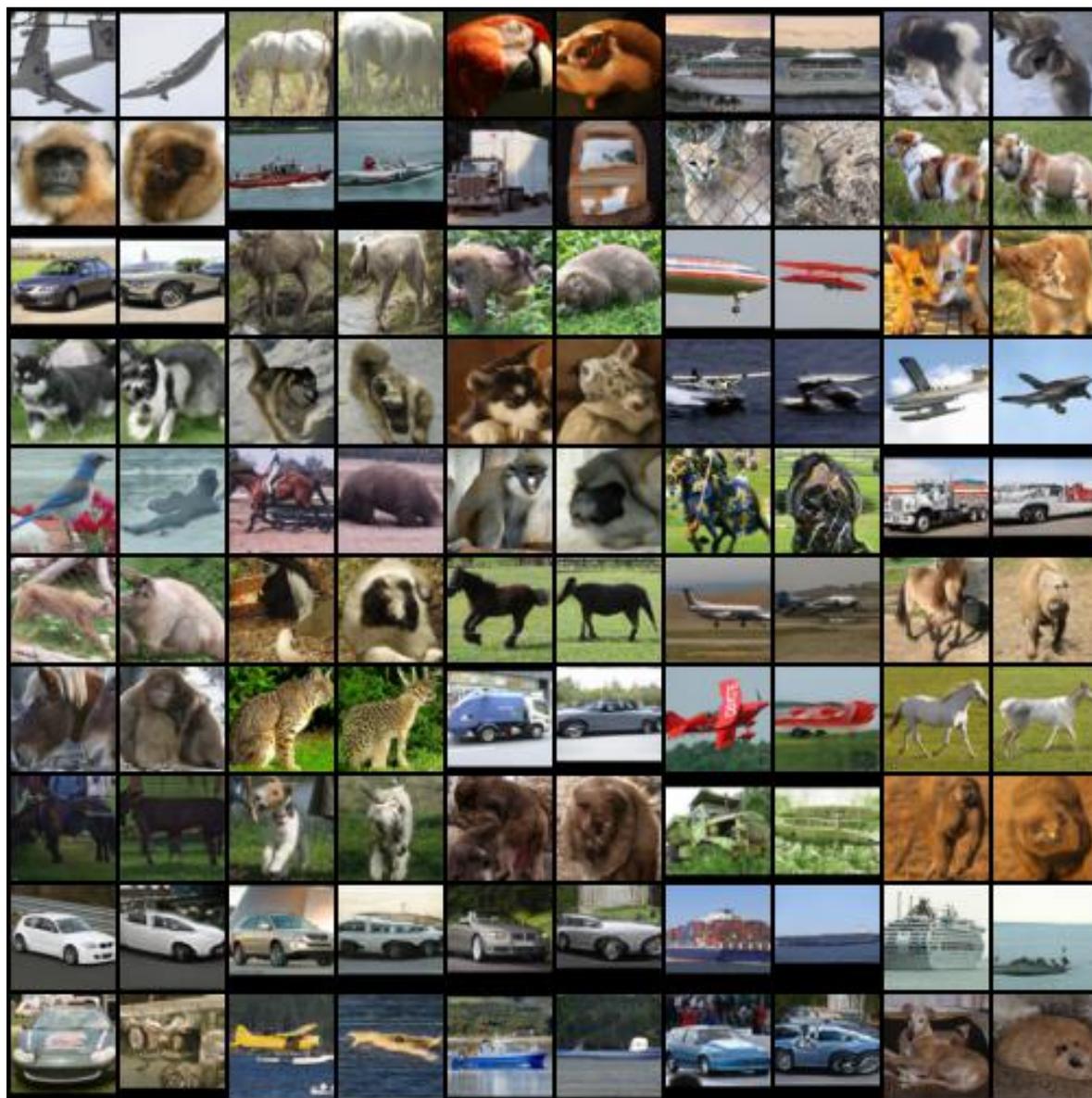


Figure 5: Encoder-generator STL10 48x48 image reconstruction. Even columns contain the original images, odd contain reconstructions. Random sample.

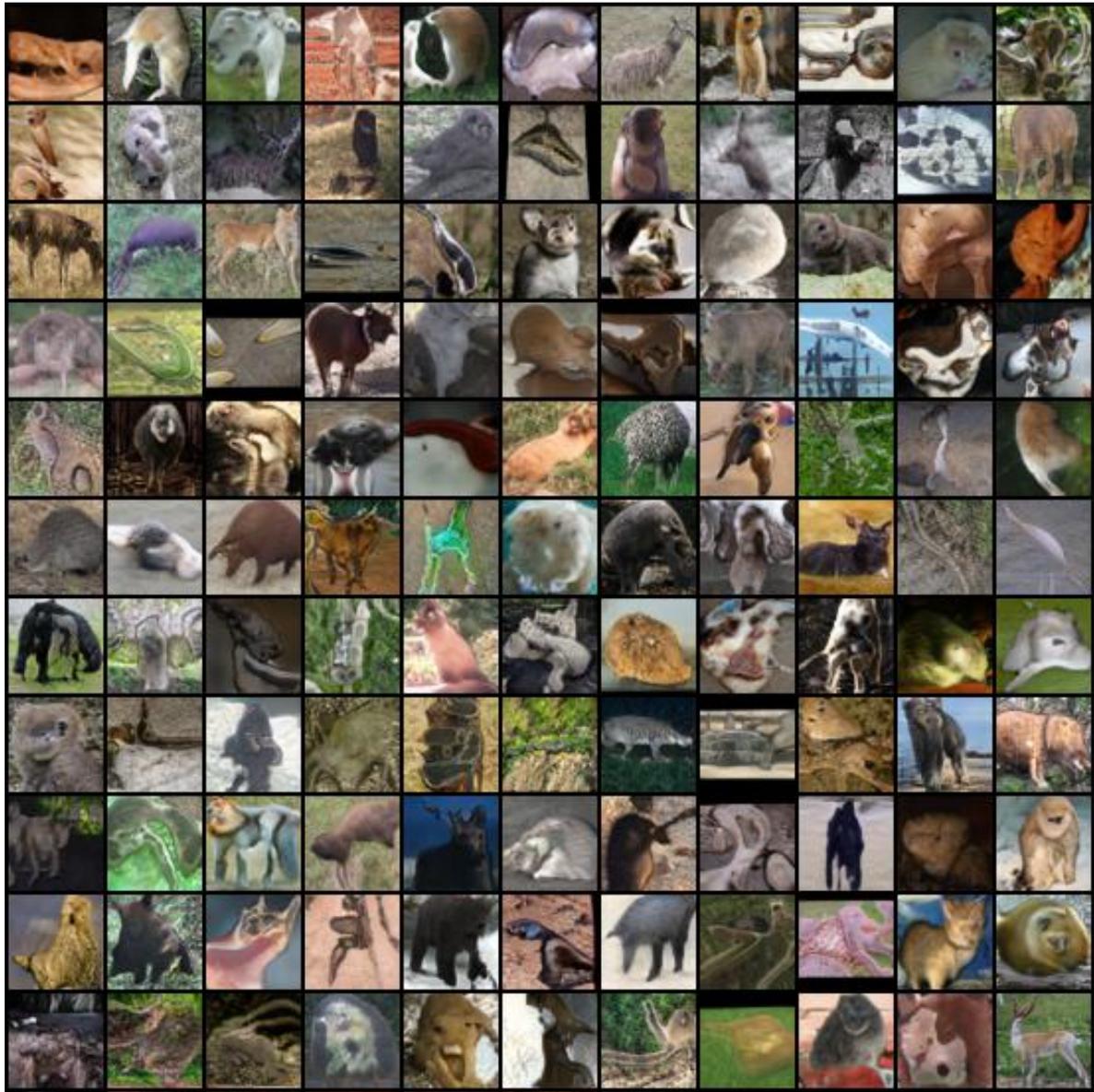


Figure 6: STL10 48x48 image generation with baseline. Randomly sampled. Compare to Figure 7.

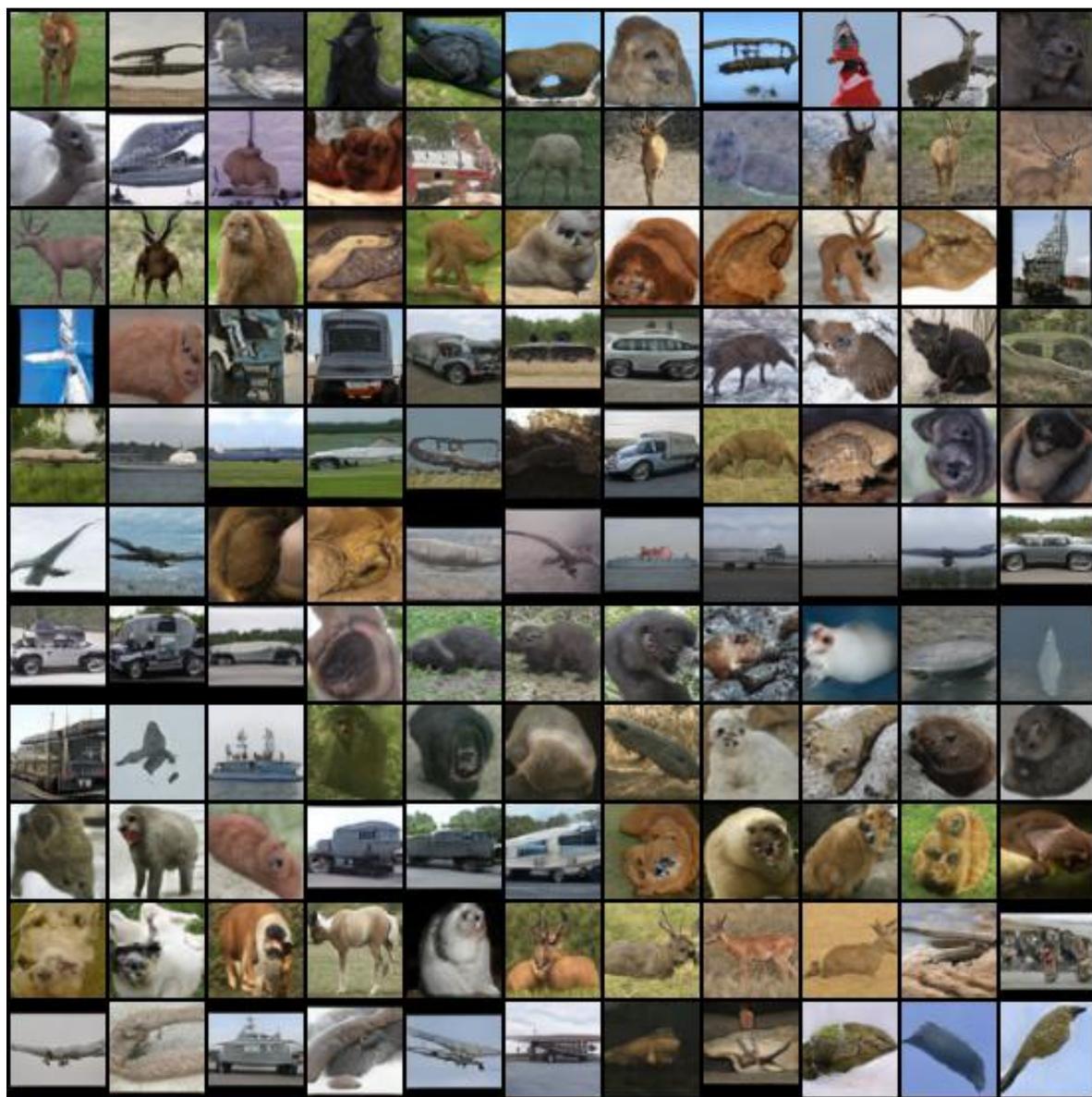


Figure 7: STL10 48x48 image generation with GAEL. Randomly sampled. Compare to Figure 6.



Figure 8: Encoder-generator CIFAR10 image reconstruction. Even columns contain the original images, odd contain reconstructions. Random sample.



Figure 9: CIFAR10 image generation with baseline. Randomly sampled. Compare to Figure 10.



Figure 10: CIFAR10 image generation with GAEL. Randomly sampled. Compare to Figure 9.



Figure 11: Encoder-generator CIFAR100 image reconstruction. Even columns contain the original images, odd contain reconstructions. Random sample.



Figure 12: CIFAR100 image generation with baseline. Randomly sampled. Compare to Figure 13.



Figure 13: CIFAR100 image generation with GAEL. Randomly sampled. Compare to Figure 12.



Figure 14: Encoder-generator CelebA image reconstruction. Even columns contain the original images, odd contain reconstructions. Random sample.



Figure 15: CelebA image generation with GAEL. Randomly sampled.



Figure 16: Encoder-generator MNIST image reconstruction. Even columns contain the original images, odd contain reconstructions. Random sample.



Figure 17: MNIST image generation with GAEL. Randomly sampled.